Article:

Papananias, M., McLeay, T.E., Mahfouf, M. orcid.org/0000-0002-7349-5396 et al. (1 more author) (2019) A Bayesian framework to estimate part quality and associated uncertainties in multistage manufacturing. Computers in Industry, 105. pp. 35-47. ISSN 0166-3615

https://doi.org/10.1016/j.compind.2018.10.008

Computers in Industry 105 (2019) 35–47

Contents lists available at ScienceDirect

Computers in Industry

journal homepage: www.elsevier.com/locate/compind

A Bayesian framework to estimate part quality and associated uncertainties in multistage manufacturing

Moschos Papananias[a,*], Thomas E. McLeay[b], Mahdi Mahfouf[a], Visakan Kadirkamanathan[a]

[a] Department of Automatic Control and Systems Engineering, The University of Sheffield, Sheffield, UK
[b] Advanced Manufacturing Research Centre with Boeing, The University of Sheffield, Rotherham, UK

ARTICLE INFO

Article history:
Received 9 May 2018
Received in revised form 3 October 2018
Accepted 30 October 2018
Available online xxx

Keywords:
Multistage Manufacturing Process (MMP)
Bayesian inference
Regression
ANOVA
Metrology informatics
Measurement uncertainty

ABSTRACT

Manufacturing is usually performed as a sequence of operations such as forming, machining, inspection, and assembly. A new challenge in manufacturing is to move towards Industry 4.0 (the fourth Industrial revolution) concerning the full integration of machines and production systems with machine learning methods to enable for intelligent multistage manufacturing. This paper discusses Multistage Manufacturing Processes (MMPs) and develops a probabilistic model based on Bayesian linear regression to estimate the results of final inspection associated with comparative coordinate measurement given in-process measured coordinates. The results of two case studies for flatness tolerance evaluation demonstrate the effectiveness of the probabilistic model which aims at being part of a larger metrology informatics system to be developed for predictive analytics and agent-based advanced control in multistage manufacturing. This solution relying on accurate models can minimise post-process inspection in mass production with independent measurements.

1. Introduction

Manufacturing concerns the application of many kind of machinery and tools to ensure product quality and functionality. Dedicated machines to manufacturing tasks may add value to parts by changing their form and properties or ensure their conformance to design specifications. Data acquisition systems are employed to provide raw data associated with the state of the production processes. A manufacturing process usually involves multiple operations to produce accurate products with the desired properties and a high level of confidence. Therefore, the performance of each operation and thus part quality is influenced by a large range of error sources induced by the current as well as preceding operations. A typical production process for metallic products consists of metal forming, subtractive machining, inspection, assembly and testing. Following the manufacture, the product will have an in-service life. Each of these steps may be important to consider. Briefly, further detail of these process steps is now discussed. Fig. 1 shows the product development process consisted of five operations or workstations; forming workstation, machining workstation, inspection workstation, assembly workstation and test workstation.

Metal forming: A given starting material is formed, cast, rolled, or perhaps additively manufactured. Heat treatment, quenching and tempering may be an important part of the material forming given that it can significantly affect the properties of the material, such as strength and stress distribution, and therefore the performance of the final product. Heat treatment is the process of heating and cooling materials to modify their microstructure and mechanical properties and thus, also affecting machinability.

Machining: Most machining operations (milling, turning, drilling, etc.) are accomplished using Computer Numerically Controlled (CNC) machine tools. These machines are among the most accurate of all production machines used in manufacturing industry. They have been studied extensively over the last decades to reduce manufacturing errors and variability [1].

Inspection: The actual shapes of most manufactured parts are obtained by Coordinate Measuring Systems (CMSs) such as Coordinate Measuring Machines (CMMs) though comparator gauges have also been recently applied to dimensional inspection, mainly, for shop floor inspection tasks. Although such devices only record point coordinates on the part surface, they are very flexible as they are equipped with tolerance assessment software.

Assembly: The assembly of parts is often performed by robots usually equipped with vision systems. The dimensional accuracy

* Corresponding author.
E-mail addresses: m.papananias@sheffield.ac.uk (M. Papananias), t.mcleay@amrc.co.uk (T.E. McLeay), m.mahfouf@sheffield.ac.uk (M. Mahfouf), visakan@sheffield.ac.uk (V. Kadirkamanathan).

https://doi.org/10.1016/j.compind.2018.10.008
0166-3615/

Fig. 1. Production process stages.

and surface quality of parts are important since they affect the assembly operation and product performance. Assembly processes may vary including welding, brazing, soldering and mechanical fastening [2].

Test: The final products may be tested by a certain method to assess how well they operate. These tests differ from dimensional inspection procedures as well as mechanical and chemical tests.

In-service life: The in-service life of products is subject to various factors including its manufacturing method as well as its proper use as defined by the manufacturer.

In order to apply informatics to this problem, the multistage process must be derived numerically. Given physical constraints and based on the machining strategy, the machine tool will be capable of producing p number of parts $\boldsymbol{q}$ at time t, such that $q_j \in \boldsymbol{S}$, for all $j = 1, \ldots, p$, and $\boldsymbol{S} \subset \boldsymbol{\Omega}$. Each part is inspected by an inspection device such as a CMM, or in this case the Equator Gauge which uses a specific Compare method such as the Golden Compare or the CMM Compare [3]. The former implies that the comparator gauge is calibrated using a reference master part q^*, where $q^* \notin \boldsymbol{S}$. Therefore, any deviation of the master part to drawing nominals will be included in the measurements. The latter suggests that any production part produced close to drawing nominals can be used as a master part, where $q^* \in \boldsymbol{S}$, in this case, and therefore, it is first measured by an accurate measuring system such as a CMM. However, in both cases, the measurement uncertainty for a given production part will inherit uncertainty from the calibration of the master part.

On-Machine Measurement (OMM) may take place for rapid verification before post-process inspection. OMM can be considered as part of the machining stage as the measurements are taken with the product in situ. Products are assembled from a specific number of parts in a predefined sequence at the assembly workstation. Assembly robots are used for the joining of multiple parts. Finally, each assembled product is then tested in the last workstation.

This paper is concerned with manufacturing systems and the problem of estimating the results of final inspection from direct and/or indirect in-process monitoring data. Fig. 2 is a graphical abstract of this work where a universal metrology informatics system receives process and workpiece data and controls a MMP. Multi-Agent Systems (MASs) are proposed for the efficient automated implementation of this scheme. Under this framework, machines and production systems will be capable of sharing data and information, detecting manufacturing errors and poor quality in machined parts, and taking corrective actions to minimise part variation and propagation. This will also lead to manufacturing flexibility to product design changes and other functionalities such as autonomous self-calibration without additional efforts. MASs can realise autonomous control and synchronisation and therefore, they can be considered as an attractive solution to developing and implementing a universal metrology informatics system in accordance with Industry 4.0 principles including big data analytics (the modelling and analysis of data characterised by high volume, velocity and variety), energy efficient manufacturing, etc. [4–7]. Such an evolution requires the development of efficient predictive models. This work presents a Bayesian linear regression model to estimate the results of post-process inspection from in-process monitoring data. The Bayesian approach to statistical inference has re-emerged due to the extreme advances in computing technology and demand in many fields of science and engineering for developing more realistic models for complex phenomena and multi-parameter systems or processes.

Section 2 presents the background of the research. Section 3 presents the probabilistic model used to estimate part quality and associated uncertainties given in-process monitoring data. Sections 4 and 5 validate the proposed model using MATLAB. Finally, concluding remarks are given in Section 6.

2. Background

Metal alloys can be shaped into useful products by bulk-metal forming processes such as forging, rolling, extrusion, and drawing or sheet-metal forming processes such as bending, stretch forming, deep drawing, and spinning. Compared to metal casting and machining, metal forming provides components with superior mechanical properties but it is limited to the manufacture of less complex shapes [8,9]. The quality of a forming process is subject to many factors including: heat treatment of the material, temperature of the deformation process, strain and strain rate, lubrication and lubricant type and quality, geometry and surface properties of

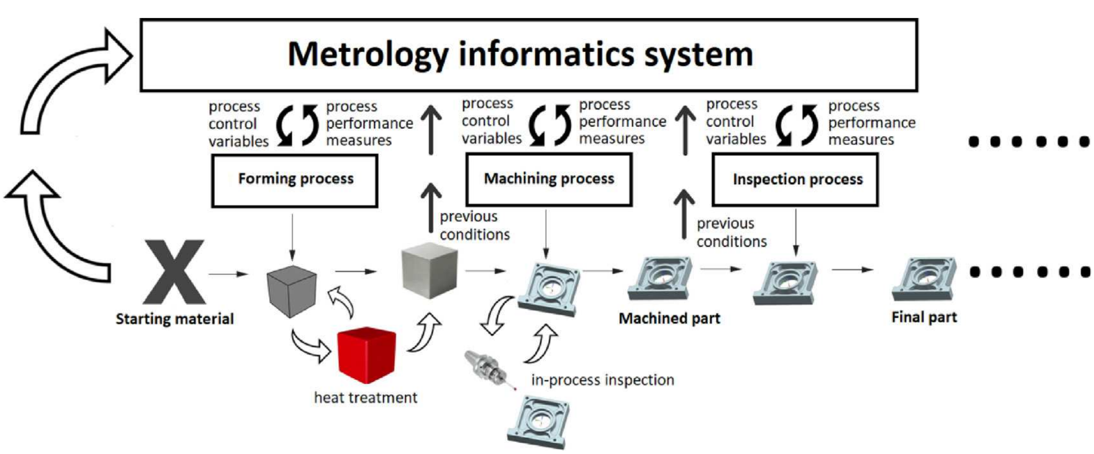

Fig. 2. Metrology informatics system.

the initial workpiece, flow stress and workability/formability of the material, tool material, tool geometry, tool wear, and shear stress though friction is controlled through lubrication. Recent developments in metal forming have led to Sheet-Bulk Metal Forming (SBMF) used for the manufacturing of sheet metal parts with functional features [10]. Casting is a manufacturing process of pouring or injecting molten material into a mold which contains it in the desired shape during solidification. Metal casting performance is mainly subject to the material, method used, pouring temperature, pouring rate, path of flow, use of chills, and risering. The physical and sometimes chemical properties of a part in a MMP are subject to changes throughout the different production steps. Four basic engineering materials can be distinguished in terms of their physical and chemical properties: metals, ceramics, polymers, and composites though composites are nonhomogeneous mixtures of the other three basic types rather than a unique category [2]. The physical properties of the part often influence the performance of the manufacturing process. For example, in machining, the thermal properties of the workpiece determine the cutting temperature and thus, affecting tool life. Tool wear or breakages have a large influence on machining processes because it leads to tool failure, machining errors of a workpiece, and unscheduled machine downtime on the shop floor [11]. In particular, the accuracy of the machined parts depends on many factors including machine geometry and thermal errors, vibration, cutting forces, feed rate, cutting and spindle speed, depth of cut, workpiece dimensions and roughness, workpiece holding method/clamping, tool type and wear, datum, and coolant type.

Although fabrication processes are designed with high criteria in order to produce efficiently high-quality parts, deviations from nominal are often found during inspection and a decision must be taken on whether or not the part meets its design specifications. However, this is not straightforward since the features are constructed using a finite number of contact points which are often limited to reduce inspection cycle times and thus, the entire geometry of the part is not known [12,13]. Also, all the measurement systems and processes are influenced by various influencing factors including usually both random and systematic effects. Therefore, it is necessary to evaluate the associated measurement uncertainties [14–16]. Evaluating the measurement uncertainties associated with complex multipurpose measuring systems such as CMMs however is difficult and many efforts are often required to achieve valid measurement uncertainty statements. In particular, the accuracy of inspection results obtained by CMSs such as CMMs is based on many factors including temperature, the probing system and machine itself, measurement part, fixturing, measurement strategy, and evaluation algorithms and filters [17,18]. The measurement strategy usually concerns the number and distribution of contact points (in discrete-point probing mode) or scanning speed and sampling point density (in scanning mode) as well as the selection of datum features and part-alignment technique. In this work, a Parallel Kinematic Machine (PKM)-based flexible gauge is considered as the measurement/gauging system for the final inspection. This device is a CMS that employs the Comparator principle to account for the influence of systematic effects associated with the measurement system [3,19–21]. Hence, the complexity of evaluating the measurement uncertainties associated with CMSs operating in absolute mode is largely reduced since many of the systematic effects associated with the measurement system cancel out. The accuracy of comparator measurement results depends on the calibration of the master part and its quality, machine repeatability, fixturing variability and part misalignment from rotation between master and measure coordinate frames, measurement strategy, measurement part, software errors, and frequency of re-mastering process and variability of temperature conditions of the shop floor environment.
On-Machine Probing (OMP) is often used for rapid verification of the machine and part [22]. However, this inspection approach is characterised by high measurement uncertainties because the same errors that influence the machining process are also transferred to the inspection process. Thus, this inspection approach may be not reliable especially for parts with tight tolerances due to the fundamental metrological limitations. CNC machine tools used as CMMs will have the same errors sources as CMMs with differences in the relative magnitude and dynamics of those errors [23]. Despite these disadvantages, OMP has been used extensively as part of the machining cycle to avoid or reduce hard gauging. Fig. 3 depicts the major error sources associated with a MMP. These error sources influence part quality and contribute to the uncertainties associated with it. As can be seen from Fig. 3, many uncertainty sources can arise from the operator e.g. measurement or machining strategy, part misalignments and fixturing.

The factory of the future requires smart, flexible, and adaptive manufacturing lines capable of being autonomously self-healed, self-adapted, and reconfigurable against product requirements changes. This requirement is known as the ‘batch-size-of-one’ (BSo1) problem. However, many factories cannot replace their existing equipment with the state of the art equipment. Sanderson et al. [24] presented an assembly cell demonstrator, called Smart Manufacturing And Reconfigurable Technologies (SMART) demonstrator, to address this challenge by applying adaptive multi-agent control to existing equipment. The demonstrator cell consists of various workstations controlled by Programmable Logic Controllers (PLCs). The ‘legacy’ system, which was requiring manual reprogramming of each PLC and sometimes physical reconfiguration when adding new recipes, was transformed to ‘SMART’ by adding an agent control layer. The SMART demonstrator was based on HAS-200 and their agents were programmed in Java Agent Development framework (JADE). The hardware for the SMART demonstrator is detailed by Chaplin et al. [25]. In particular, modern manufacturing systems adopt multi-agent technology because they include a variety of components (PLCs, machines, robots, conveyors, etc.) from different manufacturers [26,27]. Antzoulatos et al. [28] presented a multi-agent architecture to enable plug and produce based configuration and reconfiguration of assembly systems. The MAS was implemented using the communication infrastructure of JADE because of its peer-to-peer agent communication and functionality to create, execute, manage and terminate agents. An agent is an autonomous and flexible computational problem-solver capable of sensing and acting upon its environment. MASs consist of intelligent agents interacting with each other and are composed of at least two agents [29]. Holonic manufacturing systems has also received a lot of attention in recent years. A holon is a special type of an agent. Although holonic and MASs share similar concepts, holonic systems is a manufacturing-specific approach applied to achieve distributed intelligent manufacturing control while MASs is a broad software approach [30]. To minimise manufacturing errors and increase manufacturing system capabilities, many research efforts are focused on enabling machines and production systems exchange data and information. Due to the complexity of the manufacturing system consisting of various complex processes, autonomous control systems are required. Therefore, MASs can be considered as an attractive automated solution to developing and implementing a metrology informatics system. Decentralized and distributed control schemes such as MASs can provide an efficient solution for implementing the metrology informatics system since they are inherently modular, able to provide robust solutions with redundant agents, can utilise artificial intelligence techniques and handle interactions. In this case, the manufacturing equipment and systems, critical machine components, products, and other resources shall be defined as intelligent agents and communicate

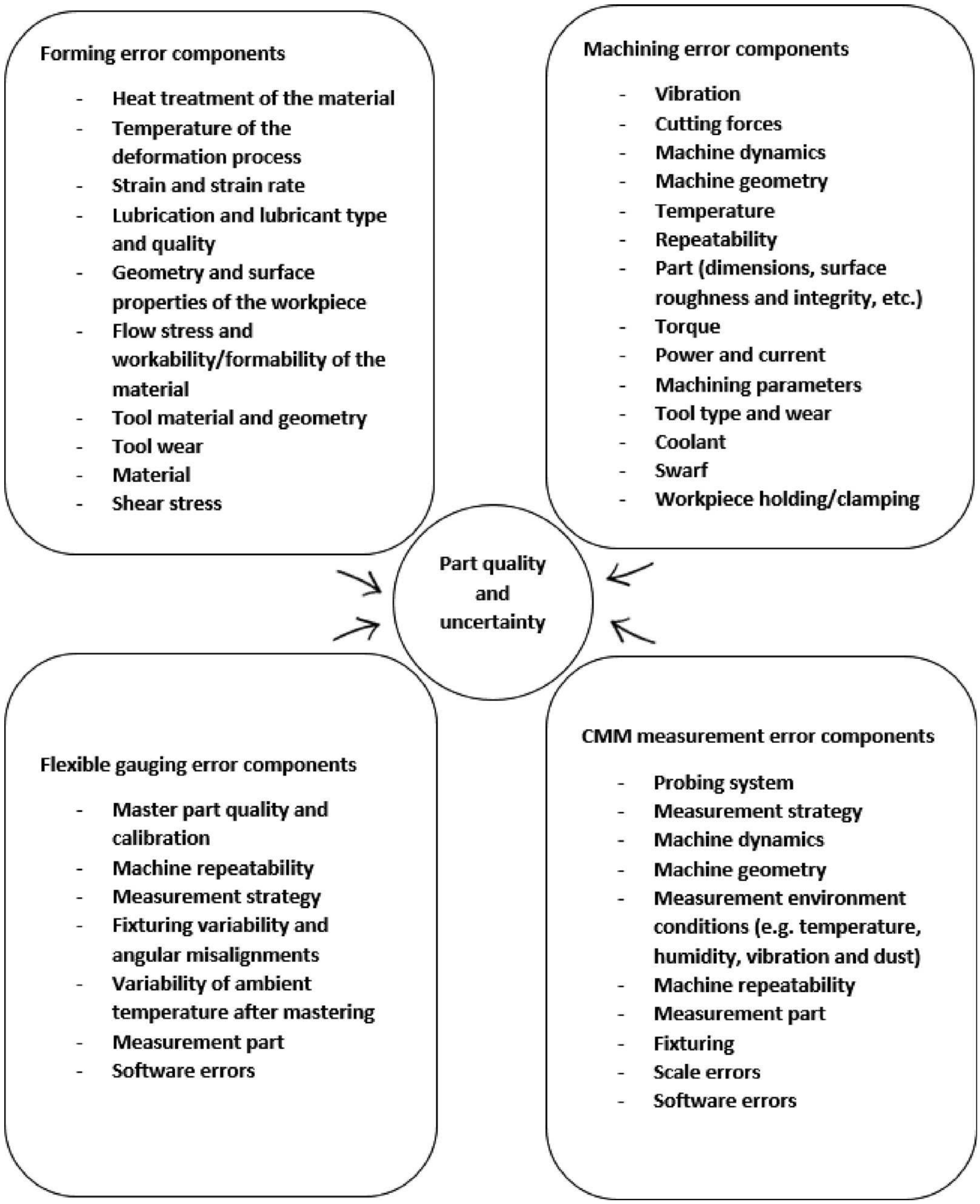

Fig. 3. MMP uncertainty contributors.

their state to the "metrology system". Then, agents for the models and simulation tools will enable actuator agents to perform an action e.g. to reduce the feed rate due to the high magnitude of vibration signals or to perform a calibration due to the high uncertainties associated with the machine axes.

Modelling MMPs has been studied extensively over the past several years. Various approaches have been proposed to reduce process variability while ensuring product quality specifications. Du et al. [31] developed a Markov model to analyse product quality propagation in multistage manufacturing systems with Remote Quality Information Feedback (RQIF). Bowling et al. [32] employed a Markovian approach to determine the optimal process target levels for MMPs. Pepyne & Cassandras [33] described a hybrid system modelling framework for MMPs by formulating and solving optimal control problems. Jiang et al. [34] proposed a machining error propagation model based on complexity network theory and Artificial Neural Networks (ANNs). An ANN is a computational model capable of acquiring, storing and utilising knowledge gained from experience [35,36]. ANNs are one of the most important components of Industry 4.0. They have been inspired by biological neural networks found in humans. The most popular ANNs are the Multi-Layer Perceptron (MLP) networks which use the Back-Propagation (BP) learning technique for training. They are known as supervised networks because a desired output is required for training the network. Mathematical models such as state space models have also been widely used in many applications including MMPs [37]. The methodology used to model variation propagation in a MMP using a state space representation is known as the Stream of Variation (SoV). Ding et al. [38] were concerned with state space modelling and diagnosing fixture variation in MMPs. Du et al. [39] presented a generic framework for 3D variation propagation modelling for

Multistage Turning Processes (MTPs) of rotary workpieces. Abellán-Nebot et al. [40] expanded the process-oriented tolerancing methodology proposed by Ding et al. [41] to incorporate critical process variables such as tool wear, cost functions and quality constraints. This was achieved by applying an extended SoV model. A comprehensive review and comparison for major linearized SoV modelling methods for MMPs can be found in [42]. Lawless et al. [43] used simple regression and Analysis of Variance (ANOVA) methods for variation reduction. In the second part of this work, Agrawal et al. [44] presented methods to deal with measurement error and obtain confidence intervals for variance proportion estimates. Regression analysis is a statistical data analysis technique used to investigate the relationship between dependent and explanatory variables [45]. It is a supervised machine learning technique with major applicability in predictive analytics. Frequentist estimation methods that are usually used to estimate the unknown parameters are the least-squares and the maximum likelihood, which yield equivalent estimates for linear models that assume that the random effects are normally distributed [46]. The work presented in this paper uses a Bayesian approach to estimate the results of final inspection from in-process inspection measurements. Bayesian methods have attracted a lot of interest in recent years because they can combine easily expert knowledge with experimental data while considering uncertainty [47]. However, they require a probability distribution to be defined on the parameter space before the data are observed (prior distribution). Due to the unpredictability of temperature changes in shop floor environments and the complexity of the measurement system, a deterministic model for the measurement process is not feasible. Instead we derive a probabilistic model and use a Bayesian approach to compute posterior distribution of the unknown parameters. With advances in computing, computational Bayesian methods such as Markov Chain Monte Carlo (MCMC) are straightforward to use to generate samples from the posterior distribution of interest which may otherwise be difficult to generate samples from. MCMC methods combine Monte Carlo sampling and Markov chain theory [48,49] to draw values of unobservable data. Well-known MCMC methods include the Metropolis algorithm, the Metropolis-Hastings algorithm, and the Gibbs sampler, also called alternating conditional sampling. In particular, the latter has been found very useful in a large number of multidimensional problems [50].

3. Probabilistic model

This section will describe a proposed probabilistic model for estimating part quality (characterised by the geometrical inspection of the part after machining) from in-process monitoring data, such as OMMs, temperature of the machine, or other sensor data or information available from a process.

Modern CNC machine tools can be used to take OMMs of a product by exchanging the cutting tool for a probing system. Such a system can gather a set of m data points $\boldsymbol{D} = \{\boldsymbol{d}_i = (x_i, y_i, z_i)^{\mathrm{T}}\}_1^m$ on the workpiece surface. Geometric tolerance assessment can then be applied to the coordinate data $\boldsymbol{D}$ to determine how close the workpiece has been manufactured to its nominal, ideal geometry. The reliability of tolerance assessment depends on a number of factors such as the measurement strategy used to gather the coordinate data, the machine geometric and thermal errors, and the probing system errors.

To estimate the measurement results of final inspection from in-process monitoring data, consider a model of the form:

$$\boldsymbol{y} = \boldsymbol{X\alpha} + \boldsymbol{\varepsilon},\ \boldsymbol{\varepsilon} \in \mathrm{N}_m(0, \sigma^2 \boldsymbol{I}_m), \tag{1}$$

where $\boldsymbol{y} = (y_1, \ldots, y_m)^{\mathrm{T}}$ is the response variable, $\boldsymbol{X}$ is the $m \times (n+1)$ matrix of covariates or design matrix, $\boldsymbol{\alpha} = (\alpha_0, \alpha_1, \ldots, \alpha_n)^{\mathrm{T}}$ represents the unknown parameters describing the state of the machine, and $\boldsymbol{\varepsilon} = (\varepsilon_1, \ldots, \varepsilon_m)^{\mathrm{T}}$ represents the error term not explained by the model. Assuming that the errors are normally distributed is not questionable since most of the random effects are associated with the response variable. Note, $\boldsymbol{I}_m$ is the $m \times m$ identity matrix. The design matrix $\boldsymbol{X}$ is given by:

$$\boldsymbol{X} = \begin{bmatrix} 1 & x_{11} & x_{12} & \cdots & x_{1n} \\ 1 & x_{21} & x_{22} & \cdots & x_{2n} \\ \vdots & \vdots & \vdots & \ddots & \vdots \\ 1 & x_{m1} & x_{m2} & \cdots & x_{mn} \end{bmatrix}, \tag{2}$$

with $n + 1 < m$. Assume that $\mathbb{E}(y_i|\boldsymbol{\alpha}, \boldsymbol{X}) = \alpha_0 + \alpha_1 x_{i1} + \ldots + \alpha_n x_{in}$ and $\mathbb{V}(y_i|\sigma^2, \boldsymbol{X}) = \mathbb{V}(\varepsilon_i) = \sigma^2$. For $n = 2$ predictor variables related to the point coordinates and additional sensor data, the design matrices for $\boldsymbol{y}_x \boldsymbol{y}_y$, and $\boldsymbol{y}_z$ are given by $\boldsymbol{X}_x = \{(x_{i0}, x_{i1} = x_i, x_{i2})^{\mathrm{T}}\}_1^m$, $\boldsymbol{X}_y = \{(x_{i0}, x_{i1} = y_i, x_{i2})^{\mathrm{T}}\}_1^m$, and $\boldsymbol{X}_z = \{(x_{i0}, x_{i1} = z_i, x_{i2})^{\mathrm{T}}\}_1^m$, respectively, where $x_{i0} = 1$, $\forall i = 1, \ldots, m$, is the coefficient of the intercept. Thus, the probabilistic model can be written as

$$\boldsymbol{y}_x|\boldsymbol{X}_x, \boldsymbol{\alpha}, \sigma^2 \sim \mathrm{N}_m(\boldsymbol{X}_x\boldsymbol{\alpha}, \sigma^2 \boldsymbol{I}_m),$$

$$\boldsymbol{y}_y|\boldsymbol{X}_y, \boldsymbol{\alpha}, \sigma^2 \sim \mathrm{N}_m(\boldsymbol{X}_y\boldsymbol{\alpha}, \sigma^2 \boldsymbol{I}_m),$$

$$\boldsymbol{y}_z|\boldsymbol{X}_z, \boldsymbol{\alpha}, \sigma^2 \sim \mathrm{N}_m(\boldsymbol{X}_z\boldsymbol{\alpha}, \sigma^2 \boldsymbol{I}_m). \tag{3}$$

The response variables $\boldsymbol{Y} = (\boldsymbol{y}_x, \boldsymbol{y}_y, \boldsymbol{y}_z)$ correspond to the raw data $\boldsymbol{G} = \{\boldsymbol{g}_i = (x_i, y_i, z_i)^{\mathrm{T}}\}_1^m$ obtained by a CMS. Although working with the raw coordinate data $p = \{(\boldsymbol{d}_i, \boldsymbol{g}_i)\}_1^m$ requires algorithms for finding least-squares best-fit geometric elements to $\boldsymbol{Y}$, it lets us evaluate uncertainty contributors associated with a particular axis of the (Cartesian) machine tool.

Our primary interest is to estimate the unknown regression parameters $\boldsymbol{\alpha}$ and variance σ^2. Classical estimation approaches such as least-squares and maximum likelihood treat the parameters as fixed, but unknown quantities, rather than as random variables. In particular, in Bayesian inference, probability statements about unknown parameters $\boldsymbol{\theta}$ given data $\boldsymbol{y}$ can be obtained by a model providing the joint Probability Density Function (PDF):

$$p(\boldsymbol{\theta}, \boldsymbol{y}) = p(\boldsymbol{\theta}) p(\boldsymbol{y}|\boldsymbol{\theta}), \tag{4}$$

where $p(\boldsymbol{\theta})$ is the prior distribution and $p(\boldsymbol{y}|\boldsymbol{\theta})$ is the likelihood. The posterior density can be determined via Bayes' rule as:

$$p(\boldsymbol{\theta}|\boldsymbol{y}) = \frac{p(\boldsymbol{\theta}, \boldsymbol{y})}{p(\boldsymbol{y})} = \frac{p(\boldsymbol{\theta}) p(\boldsymbol{y}|\boldsymbol{\theta})}{p(\boldsymbol{y})}, \tag{5}$$

where $p(\boldsymbol{y}) = \int p(\boldsymbol{\theta}) p(\boldsymbol{y}|\boldsymbol{\theta}) d\boldsymbol{\theta}$ is the prior predictive distribution, which can be omitted with fixed $\boldsymbol{y}$. Therefore, the posterior density can be written in the unscaled form as:

$$p(\boldsymbol{\theta}|\boldsymbol{y}) \propto p(\boldsymbol{\theta}) p(\boldsymbol{y}|\boldsymbol{\theta}). \tag{6}$$

Given the observed data $\boldsymbol{y}$, future data $\tilde{\boldsymbol{y}}$ can be generated using for example Monte Carlo simulation. The distribution of $\tilde{\boldsymbol{y}}$, conditional on $\boldsymbol{y}$, $p(\tilde{\boldsymbol{y}}|\boldsymbol{y})$, is called the posterior predictive distribution given by:

$$p(\tilde{\boldsymbol{y}}|\boldsymbol{y}) = \int p(\tilde{\boldsymbol{y}}, \boldsymbol{\theta}|\boldsymbol{y}) d\boldsymbol{\theta}$$

$$= \int p(\tilde{\boldsymbol{y}}|\boldsymbol{\theta}, \boldsymbol{y}) p(\boldsymbol{\theta}|\boldsymbol{y}) d\boldsymbol{\theta}$$

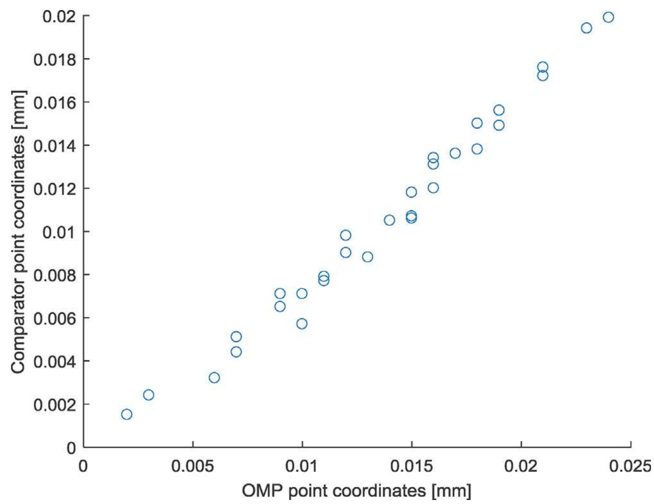

Fig. 4. Comparator data against OMP data.

$$= \int p(\tilde{\boldsymbol{y}}\,|\boldsymbol{\theta})p(\boldsymbol{\theta}|\boldsymbol{y})d\boldsymbol{\theta}, \tag{7}$$

since in this model, $\boldsymbol{y}$ and $\tilde{\boldsymbol{y}}$ are conditionally independent given $\boldsymbol{\theta}$ [48]. However, the 'data' in a regression problem include both $\boldsymbol{X}$ and $\boldsymbol{y}$. Therefore, the posterior distribution for $\boldsymbol{\theta}$, given $\boldsymbol{y}$ and $\boldsymbol{X}$, can be written as:

$$p(\boldsymbol{\theta}|\boldsymbol{y},\boldsymbol{X}) \propto p(\boldsymbol{\theta})p(\boldsymbol{y},\boldsymbol{X}|\boldsymbol{\theta}), \tag{8}$$

where $p(\boldsymbol{\theta})$ is the prior distribution representing the prior knowledge about $\boldsymbol{\theta}$ and $p(\boldsymbol{y},\boldsymbol{X}|\boldsymbol{\theta})$ is the likelihood. We assume that prior beliefs about $\boldsymbol{\theta}_{y|x}$ and $\boldsymbol{\theta}_x$ are independent [49]:

$$p(\boldsymbol{\theta}) = p(\boldsymbol{\theta}_{y|x},\boldsymbol{\theta}_x) = p(\boldsymbol{\theta}_{y|x})p(\boldsymbol{\theta}_x) = p(\boldsymbol{\alpha},\sigma^2)p(\boldsymbol{\theta}_x). \tag{9}$$

Thus, the posterior density for the unknown parameters is:

$$p(\boldsymbol{\alpha},\sigma^2,\boldsymbol{\theta}_x|\boldsymbol{y},\boldsymbol{X}) = p(\boldsymbol{\alpha},\sigma^2|\boldsymbol{y},\boldsymbol{X})p(\boldsymbol{\theta}_x|\boldsymbol{X}), \tag{10}$$

and the likelihood of the normal linear model is:

$$p(\boldsymbol{y};\boldsymbol{X},\boldsymbol{\alpha},\sigma^2) = (2\pi\sigma^2)^{-m/2}\exp\left[\frac{-(\boldsymbol{y}-\boldsymbol{X\alpha})^{\mathrm{T}}(\boldsymbol{y}-\boldsymbol{X\alpha})}{2\sigma^2}\right]. \tag{11}$$

Note that, our interest lies only with $\boldsymbol{\theta}_{y|x}$. An important issue in Bayesian inference is the selection of prior density. Using a conjugate prior density for the parameter vector $\boldsymbol{\theta}_{y|x} = (\boldsymbol{\alpha},\sigma^2)^{\mathrm{T}}$, then, the posterior density is:

$$p(\boldsymbol{\alpha},\sigma^2|\boldsymbol{y},\boldsymbol{X}) \propto p(\boldsymbol{\alpha},\sigma^2)p(\boldsymbol{y}|\boldsymbol{\alpha},\sigma^2), \tag{12}$$

where $p(\boldsymbol{\alpha},\sigma^2) = p(\boldsymbol{\alpha}|\sigma^2)p(\sigma^2)$ is the prior distribution and $p(\boldsymbol{y}|\boldsymbol{\alpha},\sigma^2)$ is the likelihood. Conjugate prior distributions for $\boldsymbol{\alpha}$, conditional on σ^2, and σ^2 can be given by:

$$\boldsymbol{\alpha}|\sigma^2 \sim \mathrm{N}_{n+1}(\mathrm{a}_0,\sigma^2\boldsymbol{V}_0^{-1}),\ \sigma^2 \sim \mathrm{IG}(a_0,b_0). \tag{13}$$

So, the conditional prior density for $\boldsymbol{\alpha}$ given σ^2 is a multivariate normal density with mean $\mathrm{a}_0 \in \mathbb{R}^{n+1}$ and variance-covariance matrix $\sigma^2\boldsymbol{V}_0^{-1}$, where $\boldsymbol{V}_0$ is a symmetric positive definite matrix of size $(n+1)\times(n+1)$, and the prior density for σ^2 is an inverse Gamma density with shape a_0 and scale b_0. Note that, while the conditional posterior density $p(\boldsymbol{\alpha}|\sigma^2,\boldsymbol{y},\boldsymbol{X})$ is a multivariate normal density, the marginal posterior density $p(\boldsymbol{\alpha}|\boldsymbol{y},\boldsymbol{X}) = \int p(\boldsymbol{\alpha}|\sigma^2,\boldsymbol{y},\boldsymbol{X})p(\sigma^2|\boldsymbol{y},\boldsymbol{X})d\sigma^2$ is a multivariate t-density [49]. In situations as in this case where prior knowledge is difficult to elicit in probabilistic form, then, for this model, a noninformative prior can be given by:

$$p(\boldsymbol{\alpha},\sigma^2) \propto \frac{1}{\sigma^2}\,. \tag{14}$$

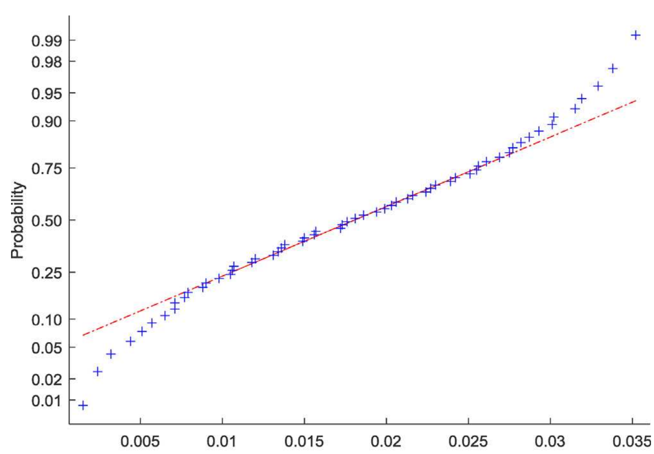

Fig. 5. Normal probability plot of the comparator data.

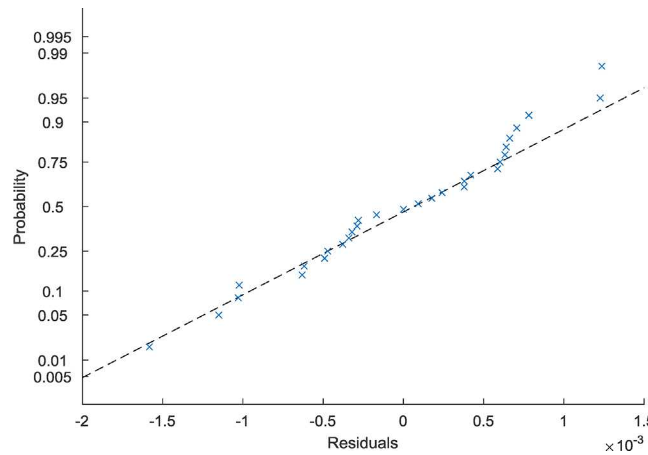

Fig. 6. Normal probability plot of residuals.

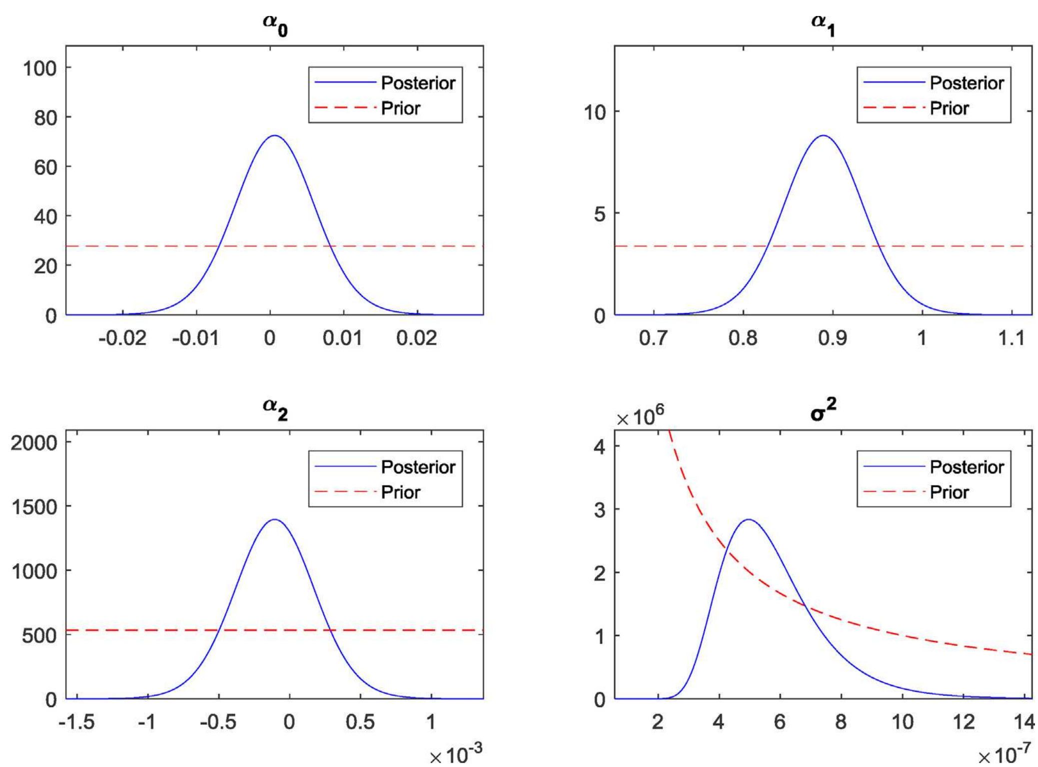

Fig. 7. Prior and posterior distributions of the parameters.

Table 1
Estimated regression parameters and disturbance variance.

	Estimate	SE	Bayesian CI	Positive	p-value
α_0	0.0006	0.0057	[-0.0106, 0.0118]	0.544	0.91
α_1	0.8893	0.0466	[0.7973, 0.9813]	1.000	1×10^{-17}
α_2	−0.0001	0.0003	[-0.0007, 0.0005]	0.356	0.71
σ^2	6×10^{-7}	2×10^{-7}	[3.3×10^{-7}, 9.9×10^{-7}]	1.000	

Table 2
ANOVA results.

	SSE [mm]	DOF	MSE [mm]
TSS	0.000717	29	0.000025
ESS	0.000702	2	0.000351
RSS	0.000014	27	0.000001

4. Model validation

This section concerns the prediction quality of the probabilistic model. Our main aim is to obtain a probabilistic model capable of predicting future response data $\tilde{\boldsymbol{y}}$ given future predictor data $\tilde{\boldsymbol{X}}$ with the minimum prediction error. To validate the model, data points $\boldsymbol{d}_l$ associated with on-machine probe coordinate data were generated according to a model of the form:

$$\boldsymbol{d}_i = w_i + \boldsymbol{\Phi}(w_i, \boldsymbol{b}) + \varepsilon_i,\ \varepsilon_i \in \mathrm{N}(0, \sigma^2),\ i \in \boldsymbol{I} = \{1, \ldots, m\}, \quad (15)$$

where w_i is the true probing point related to the workpiece surface, $\boldsymbol{\Phi}(w_i, \boldsymbol{b})$ is a deterministic error model of the system parameters $\boldsymbol{b}$ to account for the systematic effects associated with the machine,

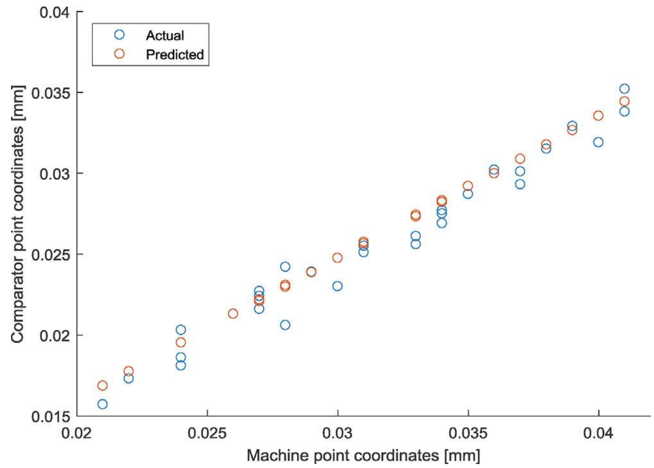

Fig. 8. Predicted model responses to new data.

and ε_i represents the random effects drawn from a Gaussian distribution with zero mean and variance σ^2. Note, $\boldsymbol{I}$ is also used to denote the identity matrix with ones on the diagonal and zeroes everywhere else. For a comparator system error used for measuring final part geometry, we considered a model of the form:

$$\boldsymbol{g}_i = w_i + e + \varepsilon_i,\ \varepsilon_i \in \mathrm{N}(0, \sigma^2),\ i \in \boldsymbol{I} = \{1, \ldots, m\}, \tag{16}$$

where w_i is the true probing point related to the workpiece surface, e represents a fixed offset associated with the comparator system, and ε_i represents the random effects [19,20].

Six data sets including ten data point coordinates each were generated. Half of the data sets were used for fitting the model and half of the data sets were used for testing it. Fig. 4 plots the comparator point coordinates $\boldsymbol{g}_i := z_i$ against the CNC machine tool point coordinates $\boldsymbol{d}_i := z_i$, for $i = 1, \ldots, 30$. Fig. 5 displays the normal probability plot of the complete data set for the comparator system. Fig. 6 shows the normal probability plot of the classical regression model residuals. As can be seen, the model residuals follow a normal distribution with small deviations from normality. For many data points and a small number of parameters the noninformative prior distribution $p(\boldsymbol{\alpha}, \sigma^2) \propto 1/\sigma^2$ offers the advantage that it provides acceptable results without the need to specify prior knowledge in the form of an informative prior. In this case, the conditional posterior density $p(\boldsymbol{\alpha}|\sigma^2, \boldsymbol{y}, \boldsymbol{X})$ is a multivariate normal density given by:

$$\boldsymbol{\alpha}|\sigma^2, \boldsymbol{y}, \boldsymbol{X} \sim \mathrm{N}_{n+1}\left(\hat{\boldsymbol{\alpha}}, \sigma^2(\boldsymbol{X}^{\mathrm{T}}\boldsymbol{X})^{-1}\right), \tag{17}$$

where $\hat{\boldsymbol{\alpha}} = (\boldsymbol{X}^{\mathrm{T}}\boldsymbol{X})^{-1}\boldsymbol{X}^{\mathrm{T}}\boldsymbol{y}$ is the Maximum Likelihood Estimate (MLE). The posterior is proper if and only if $\boldsymbol{X}^{\mathrm{T}}\boldsymbol{X}$ is nonsingular. The marginal posterior density $p(\sigma^2|\boldsymbol{y}, \boldsymbol{X})$ is an inverse Gamma density given by:

$$\sigma^2|\boldsymbol{y}, \boldsymbol{X} \sim \mathrm{IG}\left(\frac{m-n-1}{2}, \frac{(\boldsymbol{y}-\boldsymbol{X}\hat{\boldsymbol{\alpha}})^{\mathrm{T}}(\boldsymbol{y}-\boldsymbol{X}\hat{\boldsymbol{\alpha}})}{2}\right). \tag{18}$$

The marginal posterior density $p(\boldsymbol{\alpha}|\boldsymbol{y}, \boldsymbol{X})$ is a multivariate t-density with $m-n-1$ Degrees of Freedom (DOF):

$$\boldsymbol{\alpha}|\boldsymbol{y}, \boldsymbol{X} \sim \mathrm{t}_{m-n-1}\left(\hat{\boldsymbol{\alpha}}, s^2(\boldsymbol{X}^{\mathrm{T}}\boldsymbol{X})^{-1}\right), \tag{19}$$

where $s^2 = (\boldsymbol{y}-\boldsymbol{X}\hat{\boldsymbol{\alpha}})^{\mathrm{T}}(\boldsymbol{y}-\boldsymbol{X}\hat{\boldsymbol{\alpha}})/(m-n-1)$ is the sample variance. Finally, the posterior predictive distribution $p(\tilde{\boldsymbol{y}}|\boldsymbol{y})$ is a multivariate t-density with $m-n-1$ DOF:

$$p(\tilde{\boldsymbol{y}}|\boldsymbol{y}) \sim \mathrm{t}_{m-n-1}\left(\tilde{\boldsymbol{X}}\hat{\boldsymbol{\alpha}}, s^2\left(\boldsymbol{I}_m + \tilde{\boldsymbol{X}}(\boldsymbol{X}^{\mathrm{T}}\boldsymbol{X})^{-1}\tilde{\boldsymbol{X}}^{\mathrm{T}}\right)\right). \tag{20}$$

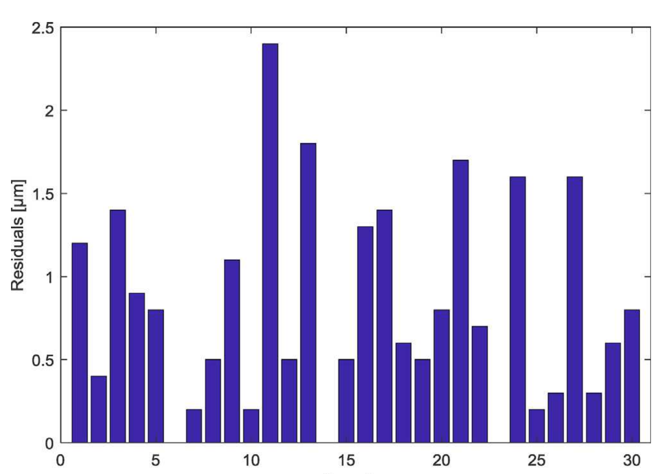

Fig. 9. Residuals.

Fig. 7 shows the prior and posterior distributions of the random regression coefficients $\boldsymbol{\alpha}$ and disturbance variance σ^2. Table 1 shows the results for the model terms. The columns of Table 1 are as follows: the first column includes the terms included in the model; the second column includes the mean value of the coefficient estimates; the third column includes the Standard Deviation (SD) or the Standard Error (SE) of the coefficients; the fourth column includes the 95% Bayesian equal-tailed Credible Interval (CI) for the parameters; the fifth column includes the posterior probability that the parameter is greater than zero; and the sixth column includes the p-value from the frequentist statistics where a term is statistically significant for 95% confidence level when the p-value < 0.05 given the other model terms. Table 2 shows the ANOVA results. The columns of Table 2 are as follows: the first column includes the Total Sum of Squares (TSS), the Explained Sum of Squares (ESS), and the Residual Sum of Squares (RSS); the second column includes the Sum of Squared Error (SSE); the third column includes the DOF; and the fourth column includes the Mean Squared Error (MSE). The coefficient of determination was $R^2 = 0.980$, the adjusted $R^2 = 0.978$, the F-statistic = 658.85, and the p-value = 1×10^{-23} for the F-test on the model. Fig. 8 shows the predicted mean responses to unseen data. Fig. 9 shows the residual values obtained by the difference between the predicted values and the expected values in order to assess the deviation of the prediction results from the expected data. The forecast Root Mean Squared Error (RMSE) was 1 μm. It can be concluded that the model predicted responses compared well against the true observations, the residual values are very small (< 2.5 μm), the model explains most of the response variable variation (high R^2 value), and that due to the use of diffuse priors the performance of the model can increase as the prior sample size increases. This was also validated by fitting the model using four data sets and testing it using the remaining two data sets. In that case, the coefficient of determination was $R^2 = 0.987$, the adjusted $R^2 = 0.986$, the F-statistic = 1398.80, and the p-value = 1×10^{-35} for the F-test on the model. The forecast RMSE from this simulation was 0.991 μm and the residual values were also less than 2.5 μm.

5. Experimental model validation

Another case was considered to validate the proposed method using experimental data. Experimental work was performed using an DMG MORI NVX 5080 3-axis machine with an OMP60 probe to obtain OMP coordinate data and a comparator system for the final inspection results. The comparative sampled points were generated based on the fitted results obtained from the comparator. The comparator system used to obtain the post-process inspection results was an Equator 300 Extended Height system. The probing

Fig. 10. Experimental setup: OMP (left); CMM measurement (middle); Comparator measurement (right).

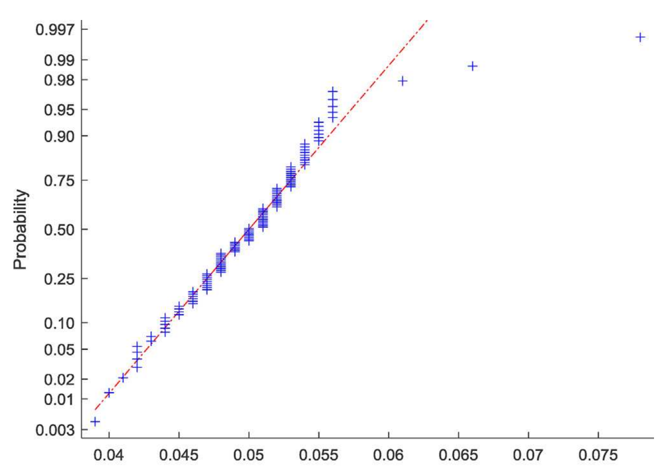

Fig. 11. Normal probability plot of the comparator data for second case study.

data correspond to points taken on the top plane of the part for flatness tolerance evaluation. The flatness tolerance defines how much a surface on a machined part may vary from the ideal flat plane. Planes are one of the most common geometric surfaces in coordinate metrology. The comparator was used in discrete-point probing mode using the CMM Compare method, which requires an accurate CMM to calibrate the master part in order to generate a calibration file for the comparator system. The calibration file was generated using a Mitutoyo CMM with REVO RSP3 probe. The calibration file is read by the comparator system during mastering to enable the probing points of a master data set to be compared with that of test data sets. The number and position of the probing points can be a major contribution to the magnitude of deviation of the machined geometry from the substitute geometry. A poor measurement strategy and a non-repeatable fixturing arrangement for a comparator system leads to large uncertainties in the computed results. The standard uncertainty associated with the fixturing repeatability in post-process inspection was very small for flatness tolerance (0.1 μm for a coverage factor of $k = 2$ and a confidence level of about 95%). The same part fixturing setup was also used for the CMM used to generate the calibration file for the comparator system. The measurement strategy used for OMP and Equator CMM Compare was the same. A general overview of the experimental setup is shown in Fig. 10.

Fig. 11 displays the normal probability plot of the complete data set for the comparator system. Note that the second validation case

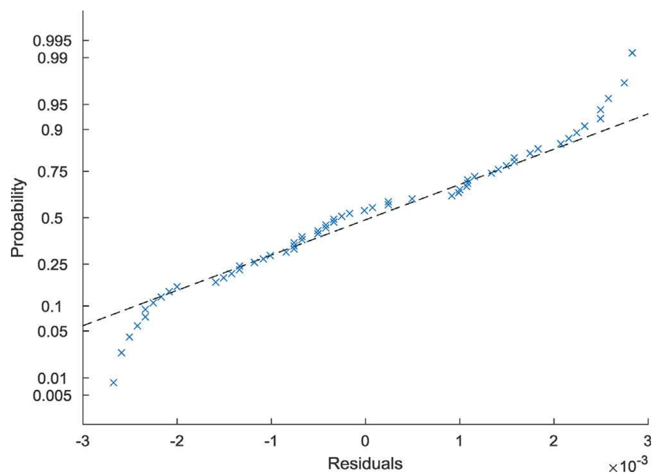

Fig. 12. Normal probability plot of residuals for second case study.

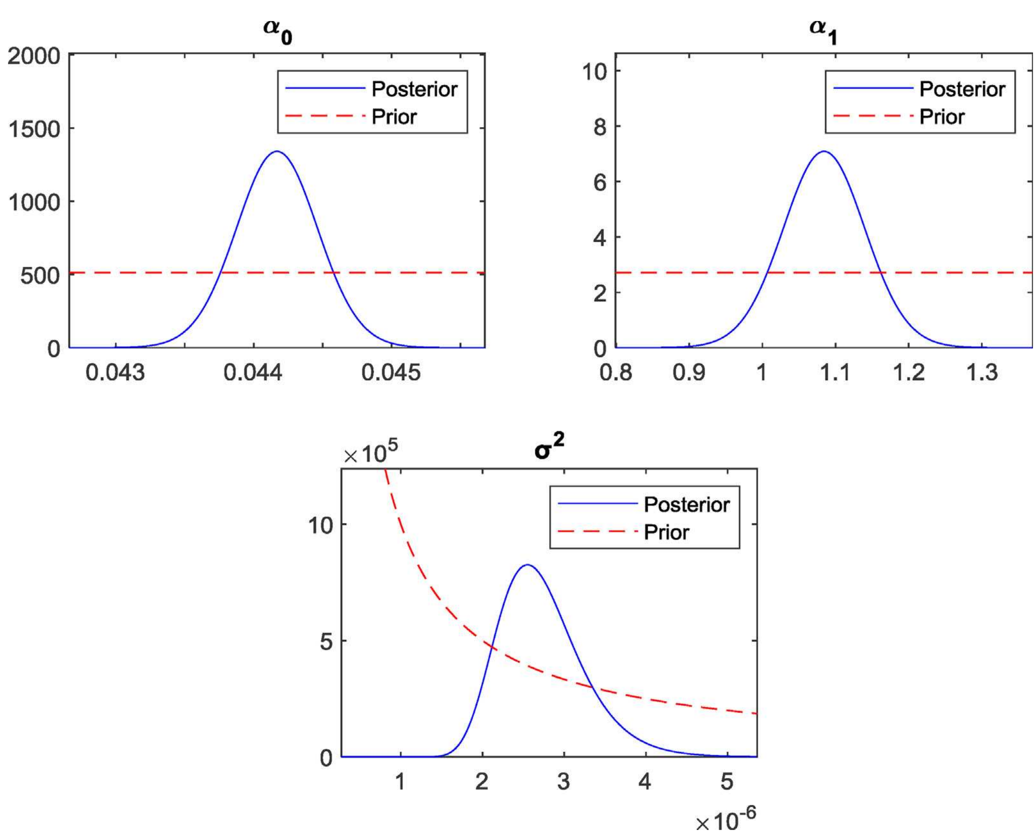

Fig. 13. Prior and posterior distributions of the parameters for second case study.

Table 3
Estimated regression parameters and disturbance variance for second case study.

	Estimate	SE	Bayesian CI	Positive	p-value
α_0	0.0442	0.0003	[0.0436, 0.0448]	1.000	1×10^{-76}
α_1	1.0842	0.0570	[0.9720, 1.1964]	1.000	6×10^{-27}
σ^2	2.7×10^{-6}	5×10^{-7}	[1.9×10^{-6}, 3.9×10^{-6}]	1.000	

Table 4
ANOVA results for second case study.

	SSE [mm]	DOF	MSE [mm]
TSS	0.001140	59	0.000019
ESS	0.000987	1	0.000987
RSS	0.000153	58	0.000003

study considers only one predictor associated with twenty OMP point coordinates for six different machined parts. Half of the data sets were used for fitting the model and half of the data sets were used for testing it.

Fig. 12 shows the normal probability plot of the regression model residuals. Fig. 13 shows the prior and posterior distributions of the unknown parameters. Table 3 shows the results for the model terms. Table 4 shows the ANOVA results. The coefficient of determination was $R^2 = 0.866$, the adjusted $R^2 = 0.863$, the F-statistic = 374.16, and the p-value = 6×10^{-27} for the F-test on the model. Fig. 14 shows the residual values. The forecast RMSE was 1.6 μm.

For comparison, an MLP neural network was developed. The ANN was trained by Bayesian regularization, which is an improvement of BP learning technique. By varying the simulations in MATLAB with different transfer functions and different numbers of hidden neurons and layers, various ANN models were developed. The MSE performance function was used to measure each network's performance. The models were trained for a different number of epochs to let the errors converge to zero. An ANN with one hidden layer, five hidden neurons, and linear activation functions were selected. The MSE was 2.7×10^{-6} mm at 1000 epochs. Fig. 15 is the bar graph of residuals obtained from the regression and ANN models, where it can be seen that both models provided similar results. Regression models are simple models and usually superior for small sample sizes. However, ANNs can easily deal with nonlinear dependencies in the data using nonlinear activation functions. The linear regression model can also be used to estimate nonlinear functions through nonlinear

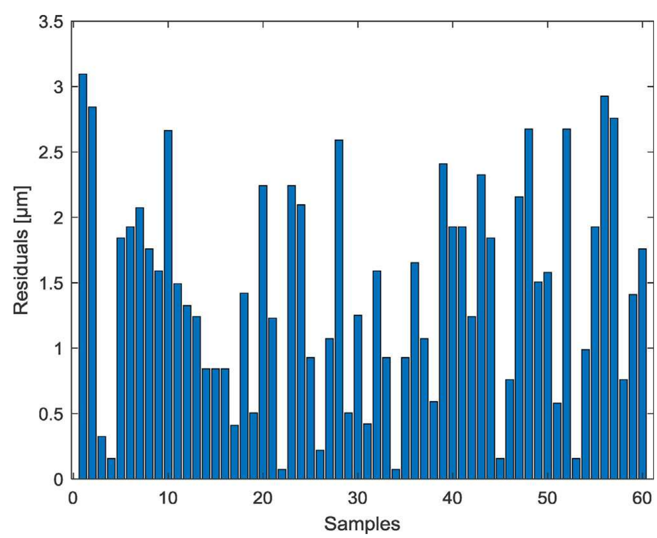

Fig. 14. Residuals for second case study.

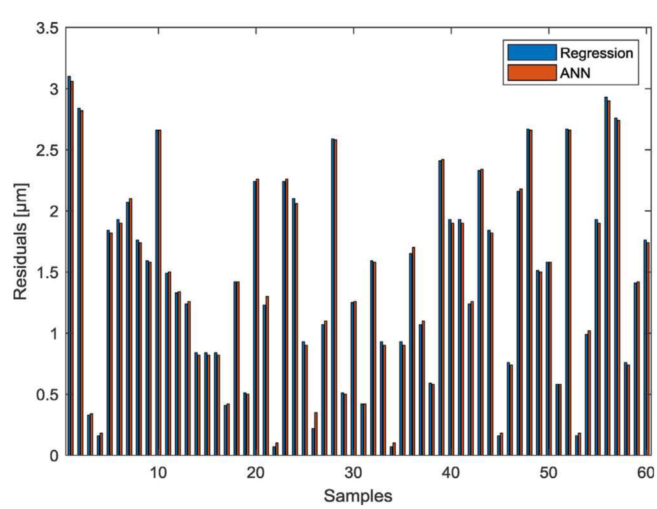

Fig. 15. Comparison of models.

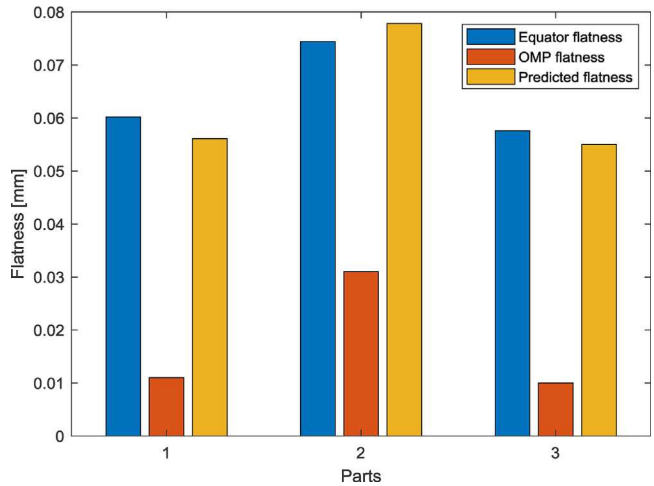

Fig. 16. Comparison of flatness values obtained from the Equator, OMP, and regression model.

transformations of data. Nevertheless, in such a case, the model will be still linear since the term linear in the linear regression models refers to the linearity of the parameters. Fig. 16 is the bar graph of flatness values obtained from the Equator, OMP, and regression model, where it can be seen that the regression model leads to much more accurate flatness estimates compared to OMP. In the case of many process variables, high sampling rates, and large measurement uncertainties, it may be necessary to pre-process the data in order to reduce the number of process variables to be used by the model. ANNs such as Self-Organising Maps (SOMs) or Principal Component Analysis (PCA) could be employed for that purpose.

6. Conclusions and future work

A manufacturing production line is a dynamic system comprised of many complex processes interacting with each other. Therefore, modelling of a Multistage Manufacturing Process (MMP) requires a sufficient understanding of all the production processes and their relationship. Due to the wide range of uncertainty sources associated with the machines and systems composing a MMP and their complex interaction, mathematical and statistical models accounting for uncertainties associated with the system model parameters are required. This paper has developed a Bayesian linear regression model to estimate part quality and associated uncertainties given in-process monitoring data. The predicted results compared well with the experimental comparator measurements for flatness tolerance evaluation. In addition, a neural network model was developed and the comparison showed that both models provided similar results.

The developed model aims to be part of a larger modular machine learning-based MMP data analytics system to be used for estimating product quality characteristics and associated uncertainties from process variables associated with the various processing stages such as heat treating, machining, and inspection. Such a system will benefit from a multivariate output including not only the part quality in terms of its dimensions and associated uncertainties but also including its mechanical, thermal, and chemical properties, all associated with stated uncertainties. The output could also include manufacturing costs, service life, and other specified parameters of interest by considering all the processes that take place during part production. Due to the new trends on the market such as customization of complex products and shorter product lifecycles, modern manufacturing faces many challenges to readjust effectively to the new requirements including big data and manufacturing intelligence. Based on real-time data, predictive analytics has the potential to create manufacturing intelligence. Despite the advancements in manufacturing metrology and data informatics, new systems and technologies are required to allow for bidirectional machine-to-machine communication and real-time computation based on efficient models and simulation tools. Within the smart factory of Industry 4.0, agent-based control has been proposed to cope with these challenges in manufacturing.

Acknowledgment

The authors gratefully acknowledge funding for this research from the UK Engineering and Physical Sciences Research Council (EPSRC) under Grant Reference: EP/P006930/1.

References

[1] Y. Altintas, Manufacturing Automation: Metal Cutting Mechanics, Machine Tool Vibrations, and CNC Design, Cambridge University Press, 2012.
[2] M.P. Groover, Fundamentals of Modern Manufacturing: Materials Processes, and Systems, John Wiley & Sons, 2007.
[3] M. Papananias, S. Fletcher, A.P. Longstaff, A.B. Forbes, Uncertainty evaluation associated with versatile automated gauging influenced by process variations through design of experiments approach, Precis. Eng. 49 (2017) 440–455.
[4] E. Hofmann, M. Rüsch, Industry 4.0 and the current status as well as future prospects on logistics, Comput. Ind. 89 (2017) 23–34.
[5] R.F. Babiceanu, R. Seker, Big data and virtualization for manufacturing cyber-physical systems: A survey of the current status and future outlook, Comput. Ind. 81 (2016) 128–137.
[6] O. Penas, R. Plateaux, S. Patalano, M. Hammadi, Multi-scale approach from mechatronic to cyber-physical systems for the design of manufacturing systems, Comput. Ind. 86 (2017) 52–69.
[7] B. Esmaeilian, S. Behdad, B. Wang, The evolution and future of manufacturing: A review, J. Manuf. Syst. 39 (2016) 79–100.
[8] H.S. Valberg, Applied Metal Forming: Including FEM Analysis, Cambridge University Press, 2010.
[9] J. Jeswiet, M. Geiger, U. Engel, M. Kleiner, M. Schikorra, J. Duflou, et al., Metal forming progress since 2000, CIRP J. Manuf. Sci. Technol. 1 (2008) 2–17.
[10] D. Gröbel, R. Schulte, P. Hildenbrand, M. Lechner, U. Engel, P. Sieczkarek, et al., Manufacturing of functional elements by sheet-bulk metal forming processes, Prod. Eng. 10 (2016) 63–80.
[11] J. Karandikar, T. McLeay, S. Turner, T. Schmitz, Tool wear monitoring using naïve Bayes classifiers, Int. J. Adv.Manuf. Technol. 77 (2015).
[12] A.B. Forbes, Measurement uncertainty and optimized conformance assessment, Measurement 39 (2006) 808–814.
[13] A. Forbes, Uncertainty associated with form assessment in coordinate metrology, Int. J. Metrol. Quality Eng. 4 (2013) 17–22.
[14] BIPM, IEC, IFCC, ILAC, ISO, IUPAC, IUPAP, OIML, Evaluation of measurement data - Guide to the expression of uncertainty in measurement, J. Comm. For. Guides Metrol., JCGM 100 (2008).

[15] A. Forbes, Approaches to evaluating measurement uncertainty, Int. J. Metrol. Quality Eng. 3 (2012) 71–77.
[16] S. Ruffa, G.D. Panciani, F. Ricci, G. Vicario, Assessing measurement uncertainty in CMM measurements: comparison of different approaches, Int. J. Metrol. Quality Eng. 4 (2013) 163–168.
[17] M. Papananias, S. Fletcher, A.P. Longstaff, A. Mengot, K. Jonas, A.B. Forbes, Evaluation of automated flexible gauge performance using experimental designs, Laser Metrology and Machine Performance XII, LAMDAMAP (2017) 45–54.
[18] R. Wilhelm, R. Hocken, H. Schwenke, Task specific uncertainty in coordinate measurement, CIRP Ann.-Manuf. Technol. 50 (2001) 553–563.
[19] A.B. Forbes, M. Papananias, A.P. Longstaff, S. Fletcher, A. Mengot, K. Jonas, Developments in automated flexible gauging and the uncertainty associated with comparative coordinate measurement, *uspen's 16th International Conference*Nottingham, UK, *E*, (2016) , pp. 111–112.
[20] A. Forbes, A. Mengot, K. Jonas, Uncertainty associated with coordinate measurement in comparator mode, Laser Metrology and Machine Performance XI, LAMDAMAP (2015) 150–159.
[21] M. Papananias, S. Fletcher, A.P. Longstaff, A. Mengot, K. Jonas, A.B. Forbes, Modelling uncertainty associated with comparative coordinate measurement through analysis of variance techniques, Euspen's 17th International Conference (2017) 407–408.
[22] F. Zhao, X. Xu, S.Q. Xie, Computer-aided inspection planning—the state of the art, Comput. Ind. 60 (2009) 453–466.
[23] P. Saunders, M. Verma, N. Orchard, P. Maropoulos, The application of uncertainty evaluating software for the utilisation of machine tool systems for final inspection, Buckinghamshire, UK, Laser Metrology and Machine Performance X, LAMDAMAP, 2013, pp. 219–228.
[24] D. Sanderson, J.C. Chaplin, L. De Silva, P. Holmes, S. Ratchev, Smart manufacturing and reconfigurable technologies: Towards an integrated environment for evolvable assembly systems, 1st IEEE International Workshop on Foundations and Applications of Self-* Systems, 2016, pp. 263–264.
[25] J. Chaplin, O. Bakker, L. de Silva, D. Sanderson, E. Kelly, B. Logan, et al., Evolvable assembly systems: a distributed architecture for intelligent manufacturing, IFAC-PapersOnLine 48 (2015) 2065–2070.
[26] A. Rocha, G. Di Orio, J. Barata, N. Antzoulatos, E. Castro, D. Scrimieri, et al., An agent based framework to support plug and produce, Industrial Informatics (INDIN), 12th IEEE International Conference, (2014) , pp. 504–510.
[27] P. Ferreira, N. Lohse, S. Ratchev, Multi-agent architecture for reconfiguration of precision modular assembly systems, Precis. Assembly Technologies Systems (2010) 247–254.
[28] N. Antzoulatos, E. Castro, D. Scrimieri, S. Ratchev, A multi-agent architecture for plug and produce on an industrial assembly platform, Prod. Eng. 8 (2014) 773–781.
[29] L. Monostori, J. Váncza, S.R. Kumara, Agent-based systems for manufacturing, CIRP Ann.-Manuf. Technol. 55 (2006) 697–720.
[30] A. Giret, V. Botti, Holons and agents, J. Intell. Manuf. 15 (2004) 645–659.
[31] S. Du, R. Xu, D. Huang, X. Yao, Markov modeling and analysis of multi-stage manufacturing systems with remote quality information feedback, Comput. Ind. Eng. 88 (2015) 13–25.
[32] S.R. Bowling, M.T. Khasawneh, S. Kaewkuekool, B.R. Cho, A markovian approach to determining optimum process target levels for a multi-stage serial production system, Eur. J. Operat. Res. 159 (2004) 636–650.
[33] D.L. Pepyne, C.G. Cassandras, Optimal control of hybrid systems in manufacturing, Proceedings of the IEEE 88 (2000) 1108–1123.
[34] P. Jiang, F. Jia, Y. Wang, M. Zheng, Real-time quality monitoring and predicting model based on error propagation networks for multistage machining processes, J. Intell. Manuf. 25 (2014) 521–538.
[35] H. Kim, M. Mahfouf, Y. Yang, Modelling of hot strip rolling process using a hybrid neural network approach, J. Mater. Process. Technol. 201 (2008) 101–105.
[36] G. Liu, V. Kadirkamanathan, Predictive control for non-linear systems using neural networks, International J. Control. 71 (1998) 1119–1132.
[37] J. Shi, Stream of Variation Modeling and Analysis for Multistage Manufacturing Processes, CRC press, 2006.
[38] Y. Ding, D. Ceglarek, J. Shi, Modeling and diagnosis of multistage manufacturing processes: part I: state space model, Proceedings of the 2000 Japan/USA Symposium on Flexible Automation, (2000) , pp. 23–26.
[39] S. Du, X. Yao, D. Huang, M. Wang, Three-dimensional variation propagation modeling for multistage turning process of rotary workpieces, Comput. Ind. Eng. 82 (2015) 41–53.
[40] J.V. Abellán-Nebot, J. Liu, F.R. Subirón, Process-oriented tolerancing using the extended stream of variation model, Comput. Ind. 64 (2013) 485–498.
[41] Y. Ding, J. Jin, D. Ceglarek, J. Shi, Process-oriented tolerancing for multi-station assembly systems, IIE Transactions 37 (2005) 493–508.
[42] F. Yang, S. Jin, Z. Li, A comprehensive study of linear variation propagation modeling methods for multistage machining processes, Int. J. Adv. Manuf. Technol. 90 (2017) 2139–2151.
[43] J. Lawless, R. Mackay, J. Robinson, Analysis of variation transmission in manufacturing processes–part I, J. Qual. Technol. 31 (1999) 131.
[44] R. Agrawal, J. Lawless, R. Mackay, Analysis of variation transmission in manufacturing processes–part II, J. Qual. Technol. 31 (1999) 143.
[45] J. Wakefield, Bayesian and Frequentist Regression Methods, Springer Science & Business Media, 2013.
[46] R. Barker, M. Cox, A. Forbes, P. Harris, Software Support for Metrology Best Practice Guide No. 4, (2004) .
[47] T. Baldacchino, S.R. Anderson, V. Kadirkamanathan, Computational system identification for bayesian NARMAX modelling, Automatica 49 (2013) 2641–2651.
[48] A. Gelman, J.B. Carlin, H.S. Stern, D.B. Dunson, A. Vehtari, D.B. Rubin, Bayesian Data Analysis, vol. 2, CRC press Boca Raton, FL, 2014.
[49] S. Jackman, Bayesian Analysis for the Social Sciences, vol. 846, John Wiley & Sons, 2009.
[50] W.R. Gilks, S. Richardson, D. Spiegelhalter, Markov Chain Monte Carlo in Practice, CRC Press, 1995.